Supramolecular effects on the antifungal activity of cyclodextrin/di-n-decyldimethylammonium chloride mixtures

Loïc Leclercq [a], Quentin Lubart [a], Anny Dewilde [b], Jean-Marie Aubry [a], Véronique Nardello-Rataj [a,*]

[a] Université Lille 1, EA Chimie Moléculaire et Formulation 4478, Equipe "Oxydation et Physico-chimie de la Formulation", Bât. C6, F-59655 Villeneuve d'Ascq Cedex, France
[b] Institut de Microbiologie, Université Lille 2, Faculté de Médecine, CHRU Lille, Bd du Professeur Leclercq, F-59037 Lille Cedex, France

ABSTRACT

Candidiasis infections are growing problem worldwide especially for the immunocompromised individuals. Di-n-decyldimethylammonium chloride is one of the most common antifungal agents used to clean medical devices. The current study examines the antifungal mechanism of di-n-decyldimethylammonium cation and its cyclodextrin inclusion complexes. Depending on the type of cyclodextrin (α-, β- or γ-**CD**), inclusion complexes can be as active as ammonium alone in terms of microorganism death (fungicidal activity). Moreover, with β-**CD** inclusion complexes, synergism is observed against fungus growth (fungistatic activity). Based on molecular dynamics, we propose a mechanism supported by cell number, selective electrode and ζ-potential measurements as a function of time. The mechanism involves four steps: (i) the positively-charged complex diffuses through the solution, (ii) it adsorbs onto the fungus membrane surface by electrostatic interaction, (iii) then it dissociates and the ammonium inserts in the microorganism membrane, and (iv) the change of the cell surface charge induces cell lysis.

© 2012 Elsevier B.V. All rights reserved.

1. Introduction

Candida albicans is a commensal fungus which lives in the human mouth and gastrointestinal tract. Under normal circumstances, *C. albicans* lives in 80% of the human population with no harmful effects. Sometimes, *C. albicans* overgrowth results in oral and genital candidiasis (Ryan and Ray, 2010; d'Enfert and Hube, 2007). Candidiasis, also known as "thrush", is a common condition, usually easily cured. However, the treatment is much more difficult in immunocompromised individuals (AIDS, chemotherapy, organ transplantation, etc.) and patients in intensive care units. In some case, Candidiasis results in septicemia. Therefore, *C. albicans*, which form biofilms on the surface of implantable medical devices, emerged as important causes of mortality in these patients. To avoid nosocomial infections, hospitals have sanitation protocols (e.g. equipment sterilization, etc.). One of the most widely used biocidal agents to clean chirurgical instruments is a double-tailed cationic surfactant: the didecyldimethylammonium chloride, [**DiC$_{10}$**][**Cl**] (Šuljagić, 2008; Russell et al., 1999), which exhibits an optimal activity in comparison with other dialkyldimethylammonium salts (Cybulski et al., 2008; Pernak et al., 2006; Pernak and Feder-Kubis, 2005; Pernak and Chwała, 2003). However, the [**DiC$_{10}$**] cation is not used alone.

Indeed, the formulation involves the use of other surfactants (e.g. polyethoxylated alcohols). In binary and multicomponent surfactant mixtures, there is a spontaneous self-aggregation which inhibits the biocidal activity due to the reduction of free [**DiC$_{10}$**] cations. To prevent this inhibition, cyclodextrins (**CDs**) can be used to form highly water-soluble complexes (Leclercq et al., 2010a,b, 2009, 2007, 2005; Leclercq and Schmitzer, 2008; Uekama et al., 1998; Funasaki et al., 2008; Jeulin et al., 2008; Kopecký et al., 2004, 2002, 2001; Lehner et al., 1993). Indeed, naturally **CDs** are six, seven or eight-membered-1,4-linked cyclic oligomers of D-glucopyranose (α-, β- and γ-**CD**) and are described as shallow truncated cones with an hydrophobic cavity (Uekama et al., 1998). Moreover, **CDs** are biocompatible and have already been used in a wide range of applications including food and pharmaceutical industries (Funasaki et al., 2008; Jeulin et al., 2008; Kopecký et al., 2004, 2002, 2001; Lehner et al., 1993). However, depending on the complex structure, the biocidal activity can be switched: encapsulated biocides can be significantly more or less active than the biocides alone (Leclercq et al., 2010a,b; Schmidt et al., 1996; Simpson, 1992). Despite a large number of publications in this field, the delivery mechanism of encapsulated [**DiC$_{10}$**] cations remains unexplored. In this article, we report on the antifungal mechanism of various **CD**/[**DiC$_{10}$**] aqueous mixtures based on *in silico* (molecular properties calculation and molecular dynamics) and *in vitro* analyses (antifungal activity against *C. albicans*, potentiometry and zetametry).

* Corresponding author. Tel.: +33 032 033 6369.
  E-mail address: veronique.rataj@univ-lille1.fr (V. Nardello-Rataj).

2. Experimental section

2.1. Materials and general information

All the reagents were purchased from Sigma–Aldrich chemicals and used without further purification. β-**CD** was a generous gift from Roquette Frères (Lestrem, France). NMR spectra were recorded in $CDCl_3$ (Euriso-top). Chemical shifts are given in ppm (δ) and measured relative to $CDCl_3$. The following abbreviations are used to explain the multiplicities: s = singlet, d = doublet, t = triplet, q = quartet, p = pentet, m = multiplet. All products were dried in a Freeze Dryer (Alpha 1-2 LD plus). In all experiments, the water used was Millipore (Simplicity 185; $\kappa = 5.5 \times 10^{-5}$ mS/m and $\sigma = 72.0$ mN m^{-1} at 20.0 °C). All measurements were taken at 20 ± 0.1 °C and repeated at least three times. Electromotive forces (emf) were measured with a Meterlab PHM250 Ion Analyzer (Radiometer Analytical) using a sensitive electrode prepared from commercial pH-glass electrode as previously reported (Collinet-Fressancourt et al., 2011; Leclercq et al., 2010a,b). For all measurements, the sensitive electrode was used in potentiometric cells in conjunction with a reference electrode of KCl-saturated calomel protected from amphiphile diffusion by a saline agar-agar gel made from 2 mol L^{-1} KCl solution contained in a Teflon capillary tube. ζ-Potentials were measured using a Zetasizer Nanosizer (Malvern). Conductance measurements were taken with a CDM210 conductivity meter (Radiometer). The optical density was measured using a UV–visible Cary 50 Probe (Varian).

2.2. Synthesis

The synthesis methodology have been previously described (see Leclercq et al., 2010a). ^{1}H NMR (300 MHz, $CDCl_3$, 25 °C, TMS): δ (ppm) = 0.85 (t, 6H; CH_3, ^{3}J = 6.9 Hz), 1.23–1.32 (m, 28H; CH_2), 1.66 (m, 4H; N–CH_2–CH_2), 3.38 (s, 6H; NCH_3), 3.45 (m, 4H; NCH_2). ^{13}C NMR (75 MHz, $CDCl_3$, 25 °C): δ (ppm) = 14.1, 22.6, 22.7, 26.2, 29.2, 29.4, 31.8, 51.3, 63.5. Anal. Calc. for ($C_{22}H_{48}$N; Cl); 9/7(H_2O): C, 68.59%; H, 13.23%; N, 3.64%; O, 5.34%; Cl, 9.20%. Found: C, 68.74%; H, 13.10%; N, 3.64%; O, 5.37%; Cl, 9.23%. m.p. = 88 °C. (Yield: 95%).

2.3. **CD**/[**DiC**$_{10}$] interaction

In order to assess the energy content of various molecules, semi-empirical quantum calculations were undertaken using the PM6-DH+ method with COSMO (conductor-like screening model) water solvation parameters as implemented in MOPAC2009^{TM} (©Stewart Computational Chemistry). The geometries are fully optimized with the PM6-DH+ semi-empirical SCF-MO method without restriction to know dispersion and H-bond energy contribution. For water simulation, a relative permittivity of 78.4 was employed with up to 92 surface segments per atom for the COSMO model being used to construct a solvent accessible surface area based on van der Waals radii. All structures were optimized to a gradient inferior to 0.1 using the eigenvector following method.

2.4. Molecular properties of free and complexed [**DiC**$_{10}$] cation

Vega ZZ 2.4.0 (© Alessandro Pedretti and Giulio Vistoli) was used to visualize and analyze the physicochemical properties (surface area, polar surface area, logP, lipole and virtual logP) of the single or complexed [**DiC**$_{10}$] cation (Pedretti et al., 2004). The lipophilic surface of single or complexed cation was calculated using the MLP surface (molecular lipophilicity potential) with the default values. MOPAC2009^{TM} was used for all others properties.

2.5. Antifungal activity

All biocidal activity tests were performed using *C. albicans* ATCC 10231. The minimum biocidal concentrations (MBC) were determined by the European standard NF EN 1275 (2006): *Chemical disinfectants and antiseptics – Quantitative suspension test for the evaluation of fungicidal activity or yeasticidal basic chemical disinfectants and antiseptics – Test method and requirements*. A sample of the product was diluted with water and a test suspension of yeast cells was added. The number of yeast cells in the suspension was adjusted between 1.5 and 5.0×10^6 cfu/mL ($6.17 \leqslant \log N_0 \leqslant 6.70$). The mixture was maintained at 20 ± 1 °C for 15 min ± 10 s. At the end of this contact time, an aliquot was taken; the biocidal activity in this portion was immediately neutralized (phosphatidylcholine 3 g, Tween 80 30 mL, sodium thiosulfate, 5H_2O 5 g, L-histidine chlorhydrate 1 g, saponin 30 g, Tryptone salt 9.5 g, water qsp. 1 L). The number of surviving yeasts in each sample was determined. Samples were serially diluted from 10^{-1} to 10^{-6} and each dilution was plated in duplicate on Agar Sabouraud Dextrose. After 48 h incubation of the plates at 37 °C, the colony-forming units par millimeter (cfu/mL) were counted. The reduction was defined as the ratio between the number of cfu/mL in the test suspension at the beginning of the contact time and the number of survivors per mL. The lowest concentration of ammonium giving a reduction of viable cells of four in a logarithm scale compared to the control was defined as the minimum biocidal concentration (MBC). The MBCs were estimated for several diluted aqueous solutions (0.1, 0.5, 1, 2.5, 5, 10, 20 and 40 v/v%) prepared from a stock solution of [**DiC**$_{10}$][**Cl**] and cyclodextrin. It is noteworthy that the [**DiC**$_{10}$][**Cl**] concentration was fixed at 1 mM (C_A) for each test but the cyclodextrin concentration was adjusted to $2.5 \times C_A$ for α-**CD** or $1.2 \times C_A$ for β- and γ-**CDs**. The minimum inhibitory concentrations (MIC) were measured using UV–visible spectroscopy. Various aqueous solutions of free or complexed ammonium were prepared. *C. albicans* was added to each solution at a concentration such that an optical density reading of 0.1–0.2 at 620 nm. The optical density readings of microorganism solutions were measured as a function of time. The MIC corresponds to the concentration at which no growth is observed. Broth containing cells alone was used as a control. The tests were repeated at least three times.

2.6. Molecular Dynamic Study

The initial configurations of **CDs** and [**DiC**$_{10}$][**Cl**] have been obtained from PM6-DH+ semi-empirical calculations. The molecular dynamic (MD) simulations were carried out in a cubic simulation box with periodic boundary conditions. In the cubic box, a phospholipid bilayer membrane model was formed with dipalmitoylphosphatidylcholine molecules. This bilayer was located between two aqueous phases. Then, a free or complexed [**DiC**$_{10}$] cation was placed in different initial relative orientations in the upper phase. An initial MD run was performed, for a period of 100 ps at 300 K with HyperChem 8.0. This solvent equilibration phase should be sufficiently extensive to enable the solvent to readjust completely to the potential field of the solute. The cutoff for non-bonded interactions was taken to be 12 Å throughout all the simulations. At the beginning, we carried out high temperature annealed MD simulations starting at 1000 K (2 ps) annealing to 0 K (100 ps). The temperature of 1000 K is necessary to enable the molecule to overcome energy barriers between different conformations and to prevent the system from getting stuck in a particular region of the conformational space. Simulations at lower temperatures yielded in very similar conformations. The simulations in aqueous solution were relaxed using the steepest descent method until a gradient different of 0.01 kcal/mol was reached. After energy minimization of the system at 0 K, the MD simulation

was initialized using a time step of 1 fs for a time period of 1000 ps. The temperature was kept constant at 300 K yielding a canonical ensemble (NVT).

3. Results and discussion

3.1. Physicochemical properties of [DiC_10] alone

[$\mathbf{DiC_{10}}$][$\mathbf{Cl}$] was obtained by a S_N2 reaction involving dimethyldecylamine and 1-decylbromide, followed by ion exchange with a hydroxide counterion and finally the aqueous solution of [$\mathbf{DiC_{10}}$][$\mathbf{OH}$] was neutralized with an aqueous hydrochloride solution (Leclercq et al., 2010a). The product was characterized by ^1H and ^{13}C NMR, and elemental analysis confirming that the salt is very pure (>99.9%) but highly hygroscopic. Thus, the salt was kept in a glove box under argon atmosphere. Before considering the antifungal properties, we have fully characterized the surfactant properties of [$\mathbf{DiC_{10}}$][$\mathbf{Cl}$] salt. To determine the CMC, [$\mathbf{DiC_{10}}$]-selective electrode have been used (Fig. 1a).

The electrode displays a pseudo-Nernstian behavior (Eq. (1)) in the concentration range from 10^{-2} and 1.7 mM, i.e. the emf linearly increases with the logarithm of the [$\mathbf{DiC_{10}}$][$\mathbf{Cl}$] concentration due to the increase of free [$\mathbf{DiC_{10}}$] concentration ([$\mathbf{DiC_{10}}$]$_{\text{free}}$). The slope (55.1 mV) is close to the value obtained for similar surfactants such as [$\mathbf{DiC_{10}}$][$\mathbf{Br}$] (58.3 mV) and suggest a pseudo-Nernstian behavior (Funasaki and Neya, 2000).

$$\text{emf} = 224.6 + 55.1 \times \log[\text{DiC}_{10}]_{\text{free}} \tag{1}$$

Above 1.7 mM, the emf decrease is due to the micellization (for more details see Leclercq et al. (2010a)). To confirm the CMC value, complementary experiments have been performed by ζ-potential measurements. As depicted in Fig. 1b, there is a significant increase of the ζ-potential just below the CMC reported above. A maximum is reached around 2.0 mM, from which, the ζ-potential decreases. It is noteworthy that the maximum (75 mV) is similar to the value reported by del Burgo et al. (2007) (73 mV). Moreover, the same profile has already been reported in the literature for dodecyltrimethylammonium bromide [$\mathbf{C_{12}}$][$\mathbf{Br}$] (Sabaté et al., 2000). Authors concluded that the maximum of the ζ-potential corresponds to the CMC and the increase below the CMC suggests the formation of pre-aggregates. We note that the CMC determined by the ζ-potential measurement is very close to the emf value (2.0 vs. 1.7 mM). The reduction of the ζ-potential above the CMC is explained by an increase in the number of the counterions adsorbed on the aggregate (Sabaté et al., 2000; Rodenas et al., 1994; Cocera et al., 1999). To confirm the adsorption of some counterions on the cationic micelles, the conductivity as a function of concentration has also been reported (Fig. 1c). We clearly observed that κ presents a break point at 1.3 ± 0.1 mM. This value is close to that obtained in the literature (1.3 vs. 1.33 mM) (del Burgo et al., 2007). Indeed, due

to the binding of some of the counterions to the aggregate, the slope in the pre-aggregation region is higher than that in the post-aggregation one. The degree of binding, β, defined as the amount of chloride counterion per micelles can be calculated according to Eq. (2) (Rosen, 2004).

$$\beta = 1 - \frac{S_{>\text{CMC}}}{S_{<\text{CMC}}} \tag{2}$$

where $S_{>\text{CMC}}$ and $S_{<\text{CMC}}$ are the slopes above and below the CMC in the κ vs. [$\mathbf{DiC_{10}}$][$\mathbf{Cl}$] concentration (C_A), respectively. From the experimental data, 40% of chlorides are bound to the cationic micelles. This value is close to the published values (Hiramatsu et al., 2003).

3.2. In vitro antifungal properties of free or complexed [DiC_10] cations

The minimal fungicidal concentrations (MBCs) and the minimal inhibitory concentrations (MICs) against *C. albicans* of aqueous solutions of [$\mathbf{DiC_{10}}$] cations with or without **CD** (α-, β- or γ-**CD**) have been determined. No activity was observed for native **CDs** alone in a concentration range from 5 to 1880 μM. In contrast, free [$\mathbf{DiC_{10}}$] cation clearly shows a biocidal activity above 79 μM thus leading to a minimum bactericidal concentration (MBC) of 79 μM (Fig. 2). This value is consistent with the literature value (Hough-Troutman et al., 2009).

As reported in the literature, the free [$\mathbf{DiC_{10}}$] cation activity is not limited to a specific class of bacteria or fungi, i.e. its spectrum biocidal activity is broad (Ferraz et al., 2011; Hough-Troutman et al., 2009; Cybulski et al., 2008; Hough et al., 2007; Pernak et al., 2006; Pernak and Feder-Kubis, 2005). However, the [$\mathbf{DiC_{10}}$] cation has a better effectiveness against *P. aeruginosa* than against *C. albicans* (55 vs. 79 μM) (Leclercq et al., 2010a). The same observations have been reported in the literature and can be explained by the nature of cell walls and cytoplasmic membranes (Russell et al., 1999). We focus here on the antimicrobial activity of **CD**/[$\mathbf{DiC_{10}}$] mixtures. The MBCs have been estimated for several diluted aqueous solutions prepared from a stock solution of ammonium (1 mM) and **CD** (2.5 eq. for α-**CD** or 1.2 eq. for β- or γ-**CD** due to their association constants, see below). A significant reduction of the antimicrobial activity (i.e. MBC increase) is obtained for the three **CD**/[$\mathbf{DiC_{10}}$] mixtures compared to free [$\mathbf{DiC_{10}}$]. However, the MBC increase by a factor two from γ-**CD** to β-**CD** to α-**CD** (85 to 176 to 345 μM) due to the decrease of the cavity size. The same behavior has been previously reported for *P. aeruginosa* (Leclercq et al., 2010a). Surprisingly, for the MIC, a minimum is observed for the β-**CD**/[$\mathbf{DiC_{10}}$] mixture whereas MIC values for α- and γ-**CD**/[$\mathbf{DiC_{10}}$] mixtures are similar to that of free [$\mathbf{DiC_{10}}$] cation. There is a synergy for the β-**CD**/[$\mathbf{DiC_{10}}$] mixture with respect to the growth of *C. albicans*. This behavior can be due to interaction of **CDs** and the phospholipids (Debouzy et al., 1998; Fauvelle et al.,
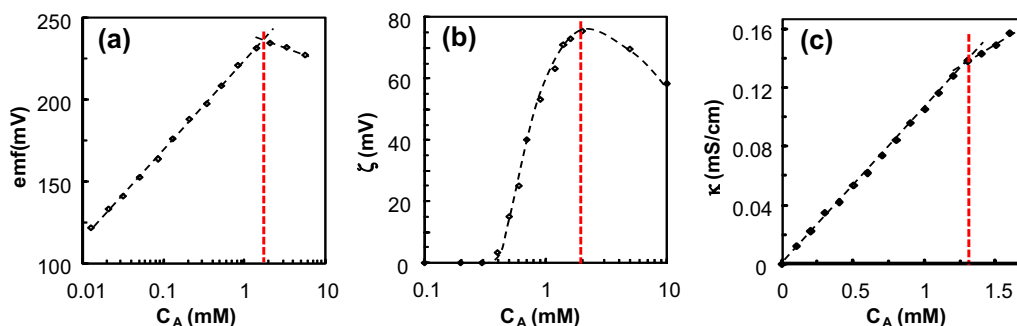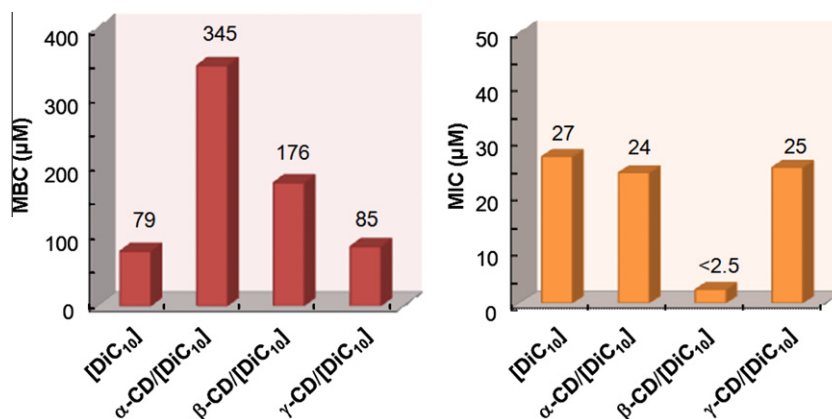

Fig. 1. Electromotive force (emf), zeta potential (ζ) and conductivity (κ) plotted against total [$\mathbf{DiC_{10}}$][$\mathbf{Cl}$] concentration (C_A) at 20 ± 0.1 °C.

Fig. 2. Minimal biocidal concentrations (MBC) and minimal inhibitory concentrations (MIC) for various **CD**/[**DiC**$_{10}$] mixtures in comparison to free [**DiC**$_{10}$] cation (2.5 for α-**CD** and 1.2 eq. for β- and γ-**CD** and). The maximum error limit of MBC and MIC measurements was ±13%.

1997). However, the control experiments performed with **CD**s alone do not show any sign of membrane damage (i.e. no cell lysis) and any reduction of the MIC in the 1–400 µM concentration range. The plausible mechanism is described in section 3.4 (see below).

3.3. Physicochemical properties of CD·[DiC₁₀] complexes

As described in our previous work, [**DiC**$_{10}$] cation easily forms inclusion complexes with various **CD**s in aqueous solution (Leclercq et al., 2010a). As the interaction energy and complex geometries are important criteria for their biocidal application, molecular modeling has been performed with the PM6-DH+ semi-empirical (Korth, 2010) method coupled with COSMO water solvation parameters as implemented in MOPAC2009™ (Klamt and Schümann, 1993). The PM6-DH+ method was parameterized to allow the description of non-covalent interactions, specifically the London dispersion energy and H-bonding while the COSMO method (conductor-like screening model) is useful for determining the stability of various species in an aqueous environment. The results are presented in Table 1 as well as the stoichiometries and the association constants determined experimentally in our previous study (Leclercq et al., 2010a). It was found that [**DiC**$_{10}$] cation exhibits

favorable interactions with all **CD**s ($E_{int} \geqslant -8$ kcal mol^{-1}). Despite 2:1 complexes are also stabilized by intermolecular H-bonds between the two **CD**s, dispersion energies are the complexation driving force. It is noteworthy that these theoretical results are supported by the experimental binding constants (Leclercq et al., 2010a).

To get a better understanding of these docked complexes, various physicochemical properties of the free or complexed [**DiC**$_{10}$] cation have been calculated from molecular modeling. As the lipophilicity can be correlated to the membrane permeation when H-bonding and electrostatic effects are not rate-determining, the octanol–water partition coefficients ($\log P$) can be easily calculated from the Broto–Moreau lipophilicity atomic constants (Zloh and Gibbons, 2007; Rahman et al., 2011). The $\log P$ of free [**DiC**$_{10}$] cation is 4.3, which suggests that it is a hydrophobic biocide which has a higher affinity for an organic phase (i.e. a biomembrane). It is apparent that upon complexation, the $\log P$ sharply decreases and the phenomenon is strongly pronounced for the 2:1 stoichiometries. As depicted in Table 1, the $\log P$ values are in the order: α-**CD**$_2$·[**DiC**$_{10}$] < β-**CD**$_2$·[**DiC**$_{10}$] < β-**CD**·[**DiC**$_{10}$] < γ-**CD**·[**DiC**$_{10}$] ≈ α-**CD**·[**DiC**$_{10}$] <<< [**DiC**$_{10}$]. However, the $\log P$ values are totally independent of the molecular geometries: the calculation is based on group contribution. Therefore, the virtual $\log P$ has been developed in the

Table 1
Interaction parameters and molecular properties of various **CD**·[**DiC**$_{10}$] complexes in comparison to free [**DiC**$_{10}$] cation.[a]

		No **CD**	**CD**·[**DiC**$_{10}$]				
			α-**CD**		β-**CD**		γ-**CD**
			1:1	2:1	1:1	2:1	1:1
Interaction parameters	Stoichiometry[b]	–	1:1	2:1	1:1	2:1	1:1
	Geometries	–					
	K (M^{-1})[b]	–	26000	7500	9700	2900	7600
	E_{int} (kcal/mol)[c]	–	−8	−51	−20	−17	−50
	E_{disp} (kcal/mol)[c]	–	−16	−31	−30	−32	−22
	E_{H-bond} (kcal/mol)[c]	–	+3	−7	+2	−8	+2
Molecular properties	$\log P$[d]	4.3	−16.5	−40.5	−21.0	−33.4	−17.5
	Virtual $\log P$[d]	5.3	−3.0	−9.8	−9.9	−6.9	−8.2
	Lipole[d]	5.4	1.8	0.6	1.2	0.8	1.3
	ΔH_{hydr} (kcal/mol)[c]	−49	−79	−100	−89	−110	−101
	%PSA[d]	0.0	37.1	43.6	51.6	40.8	38.8
	V_m (Å^3)[c]	517	1543	2512	1701	2876	1880
	Dipole (D)[c]	23.8	10.7	5.1	20.1	3.9	22.6

[a] The following abbreviation are used: K is the association constant, E_{int}, E_{disp}, and E_{H-bond}, are the interaction, the dispersion and the H-bond energies, respectively, $\log P$ is the octanol–water partition coefficient, lipole and dipole are the lipophilic and the dipole moment, respectively, ΔH_{hydr} is the hydration enthalpies, %PSA is the polar surface area coverage and V_m is the molecular volume.
[b] Taken from Leclercq et al. (2010a) from [**DiC**$_{10}$]-selective electrode at 25 °C.
[c] Based on PM6-DH+/COSMO calculation (MOPAC2009™).
[d] Calculated by the method implemented in Vega ZZ.

last decade to overcome this defect. Although the same behavior is reported for the $\log P$ and the virtual $\log P$, the decrease of this last is more moderate. The result is more realistic because the values are calculated by the projection of the Broto–Moreau lipophilicity atomic constants onto the accessible surface of complexes (Gaillard et al., 1994). The virtual $\log P$ values are in the order: β-**CD**·[**DiC$_{10}$**] ≈ α-**CD$_2$**·[**DiC$_{10}$**] < γ-**CD**·[**DiC$_{10}$**] < β-**CD$_2$**·[**DiC$_{10}$**] <<< α-**CD**·[**DiC$_{10}$**] <<< [**DiC$_{10}$**]. We have then calculated the lipophilicity distribution (Lipole) defined as the sum of local values of $\log P$ (Eq. (3)).
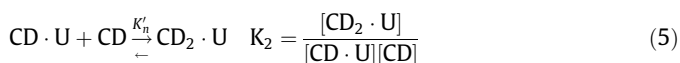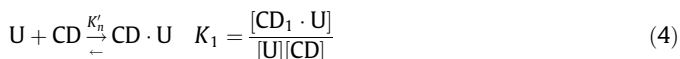
$$\text{Lipole} = \sum r_i \times l_i \qquad (3)$$

where r_i and l_i are the distance between atom i and the origin of molecule and the atomic value of the lipophilicity of atom i, respectively. The lipole is less influenced by the complexation. However, the 2:1 complexes exhibit a weak lipophilic moment compared to the 1:1 complexes: α-**CD$_2$**·[**DiC$_{10}$**] < β-**CD$_2$**·[**DiC$_{10}$**] < β-**CD**·[**DiC$_{10}$**] ≈ γ-**CD**·[**DiC$_{10}$**] < α-**CD**·[**DiC$_{10}$**] <<< [**DiC$_{10}$**]. The lipophilicity decrease upon complexation is confirmed by the hydration enthalpies (ΔH_{hydr}) and the percentage of polar surface area coverage (%PSA): it is clear that the complexed [**DiC$_{10}$**] cation presents a better affinity for water due to an increase of PSA. Moreover, the molecular volume (V_m) increases after complexation when compared to the free [**DiC$_{10}$**] cation. Finally, dipole moments are affected by the complexation: e.g. for all 2:1 complexes, a clear decrease is observed, while for the 1:1 complexes, the dipole moment remains almost constant, except for α-**CD** due to the binding of one of the two alkyl tails. As depicted in Table 1, the dipole values are in the order: β-**CD$_2$**·[**DiC$_{10}$**] < α-**CD$_2$**·[**DiC$_{10}$**] < α-**CD**·[**DiC$_{10}$**] < β-**CD**·[**DiC$_{10}$**] < γ-**CD**·[**DiC$_{10}$**] ≈ [**DiC$_{10}$**].

As reported in the literature, there is a relationship between the molecular lipophilicity and the permeability through the membrane (Mälkiä et al., 2004). So, we supposed that the complexed [**DiC$_{10}$**] are unable to pass through a biomembrane with ease (Arun et al., 2008; Loftsson et al., 2003; Stella et al., 1999; Stella and Rajewski, 1997). Indeed, lypophilicity ($\log P$, virtual $\log P$, lipole) and hydration enthalpy (ΔH_{hydr}) decrease while the polar surface area coverage (%PSA) increases. Moreover, the complexes are too large to intercalate in a biomembrane (see V_m in Table 1). However, as complexes are in equilibrium with free ammonium and as they have a potential dipole moment, we can suppose that these complexes are able to recognize the biological target (i.e. the membrane) without permeation.

3.4. In silico antifungal mechanism

For total surfactant concentrations below the CMC, the complexation takes place via a bimolecular stepwise mechanism:

$$\text{U} + \text{CD} \underset{\leftarrow}{\overset{K'_n}{\rightarrow}} \text{CD} \cdot \text{U} \qquad K_1 = \frac{[\text{CD}_1 \cdot \text{U}]}{[\text{U}][\text{CD}]} \qquad (4)$$

$$\text{CD} \cdot \text{U} + \text{CD} \underset{\leftarrow}{\overset{K'_n}{\rightarrow}} \text{CD}_2 \cdot \text{U} \qquad K_2 = \frac{[\text{CD}_2 \cdot \text{U}]}{[\text{CD} \cdot \text{U}][\text{CD}]} \qquad (5)$$

where K_n is the binding constant of the ith equilibrium, [U] and [**CD**] are the free ammonium (unimer) and cyclodextrin concentrations respectively, and [**CD$_n$**·U] is the complex concentration of the nth equilibrium. The mass balance equation for each reagent, expressed as a function of binding constants, K_1 and K_2, provides two equation systems (Eqs. (6) and (7)):

$$C_{\text{CD}} = [\text{CD}] + K_1[\text{U}][\text{CD}] + 2K_1K_2[\text{U}][\text{CD}]^2 \qquad (6)$$

$$C_A = [\text{U}] + K_1[\text{U}][\text{CD}] + K_1K_2[\text{U}][\text{CD}]^2 \qquad (7)$$

where C_A and C_{CD} are the total ammonium and cyclodextrin concentrations respectively. Combination of Eqs. (6) and (7) provides

a cubic equation (Eq. (8)) that can be solved to obtain the free **CD** concentration ([**CD**]) using Maple 12.0 (© Maplesoft).

$$K_1K_2[\text{CD}]^3 + K_1(1 + K_2(2C_A - C_{\text{CD}}))[\text{CD}]^2 + (1 + K_1(C_A - C_{\text{CD}}))[\text{CD}] - C_{\text{CD}} = 0 \qquad (8)$$

The real solution of Eq. (8) can be injected in Eq. (7) to obtain the free ammonium concentration ([U]; Eq. (9)).

$$[\text{U}] = \frac{C_A}{1 + K_1[\text{CD}] + K_1K_2[\text{CD}]^2} \qquad (9)$$

Finally, [**CD$_1$·U**] and [**CD$_2$·U**] concentrations can be calculated from the two previous solutions using Eqs. (4) and (5), respectively. As the C_{CD}/C_A ratio is fixed for each biocidal assay, the variation of [**DiC$_{10}$**] species in the **CD**/[**DiC$_{10}$**] mixtures can be calculated as a function of total ammonium concentration, C_A (Fig. 3).

As depicted in Fig. 3, for a given C_{CD}/C_A ratio, depending on the binding constants, the prevalent [**DiC$_{10}$**] species, i.e. free or 1:1 or 2:1 complexed [**DiC$_{10}$**] is clearly different. As the biocidal activity is obtained for concentrations greater than the MBC, it is possible to know the prevalent species in the active range concentration for each mixtures: (i) for α-**CD**/[**DiC$_{10}$**] mixtures, the α-**CD$_2$**·[**DiC$_{10}$**] complex is prevalent, (ii) for β-**CD**/[**DiC$_{10}$**] mixtures, the β-**CD$_1$**·[**DiC$_{10}$**] complex is in equilibrium with the β-**CD$_2$**·[**DiC$_{10}$**] one, and (iii) for γ-**CD**/[**DiC$_{10}$**] mixtures, the γ-**CD**·[**DiC$_{10}$**] species is in equilibrium with free [**DiC$_{10}$**]. Despite that complexes are probably unable to penetrate the membrane, β-**CD$_1$**·[**DiC$_{10}$**] and γ-**CD**·[**DiC$_{10}$**] complexes have similar dipole moments as the free [**DiC$_{10}$**] cation (see above, Table 1). Therefore, these two complexes are able to fix onto the fungal membrane after which the complex can be dissociated to allow the insertion of the free [**DiC$_{10}$**] cation: the complex complexes act as a reservoir of [**DiC$_{10}$**] molecules which are readily available for adsorption onto the cell. For α-**CD$_2$**·[**DiC$_{10}$**] and β-**CD$_2$**·[**DiC$_{10}$**] complexes, the antifungal activity is probably only due to the free [**DiC$_{10}$**] cations. In the presence of a biological target, the free [**DiC$_{10}$**] concentration, [**DiC$_{10}$**]$_{\text{free}}$, is in equilibrium with [**DiC$_{10}$**] adsorbed onto the cell membrane, [**DiC$_{10}$**]$_{\text{cell}}$, and with [**DiC$_{10}$**] complexed, [**DiC$_{10}$**]$_{\text{complex}}$. Therefore, the decrease of [**DiC$_{10}$**]$_{\text{free}}$, due to the insertion in the cell membrane, altering the [**DiC$_{10}$**]$_{\text{free}}$/[**DiC$_{10}$**]$_{\text{comp}}$ equilibrium and the complexed [**DiC$_{10}$**] is progressively released in solution:

$$[\text{DiC}_{10}]_{\text{complex}} \leftrightarrows [\text{DiC}_{10}]_{\text{free}} \leftrightarrows [\text{DiC}_{10}]_{\text{cell}} \rightarrow \text{cell lysis}$$
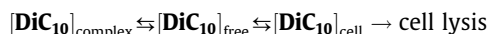
To get a better insight in the mechanism involved in the antifungal properties of free or complexed [**DiC$_{10}$**] cations, molecular modeling has been performed. The molecular dynamic (MD) simulations were carried out in a cubic simulation box with periodic boundary conditions in all directions. In the cubic box, phospholipid bilayer membrane model is formed with dipalmitoylphosphatidylcholine molecules. This bilayer is located between two aqueous phases. By convention, the upper phase represents the external environment while the lower represents the internal medium (Fig. 4).

Several 1000 ps runs were performed with different initial relative orientations of free or complexed [**DiC$_{10}$**] cations in the external phase (Fig. 4). As depicted in Fig. 5, the free [**DiC$_{10}$**] cations enter the phospholipid bilayer within the first 200 ps of the simulation run and remain in a stable position. The biocidal mechanism of free [**DiC$_{10}$**] cation is formed by three-steps: (i) diffusion in the external solution, (ii) adsorption onto the cell membrane surface by electrostatic interaction, and (iii) insertion of [**DiC$_{10}$**] cation which causes the cell lysis. This mechanism is in good agreement with the published mechanism (Denyer, 1995; Walsh et al., 2003; Obłak et al., 2001; Merianos, 2001; Balgavy and Devinsky, 1996; Ashman et al., 1986). For β-**CD$_1$**·[**DiC$_{10}$**] and γ-**CD**·[**DiC$_{10}$**] complexes, the same mechanism can be proposed. However, a
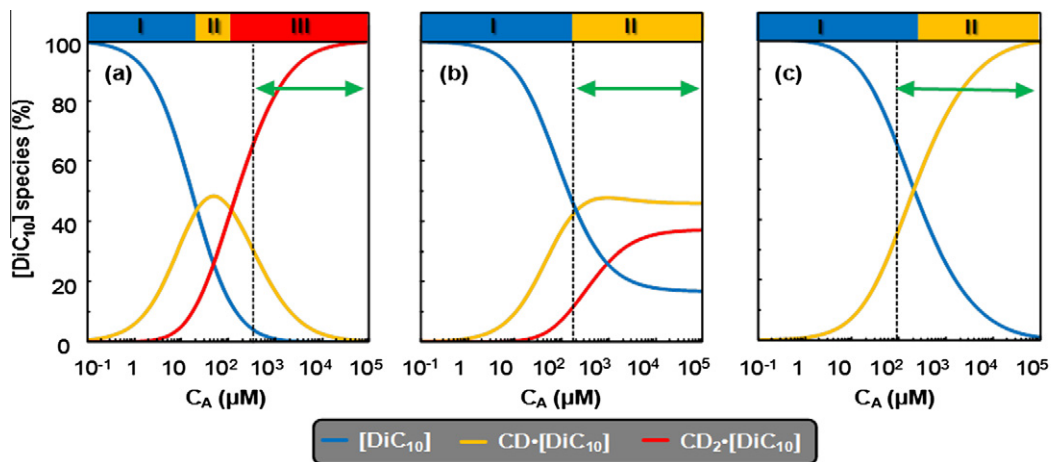
Fig. 3. Prevalent [**DiC$_{10}$**] species as a function of total ammonium concentration (C$_A$) in various **CD**/[**DiC$_{10}$**] aqueous mixtures for C$_{CD}$/C$_A$ ratio fixed in antimicrobial assay (I = free [**DiC$_{10}$**], II = **CD$_1$**·[**DiC$_{10}$**] and III = **CD$_2$**·[**DiC$_{10}$**]): (a) α-**CD**, (b) β-**CD**, and (c) γ-**CD**. The dotted line is the MBC of the **CD**/[**DiC$_{10}$**] aqueous mixture. The green double arrow represents the active concentration range active against *C. albicans*. (For interpretation of the references to color in this figure legend, the reader is referred to the web version of this article.)
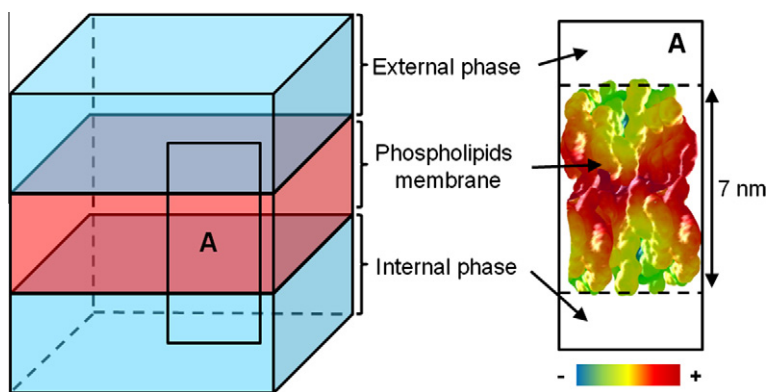
Fig. 4. Schematic representation of membrane model in a periodic box. The inset represents the membrane bilayer colored by lypophilicity (MLP surface as implemented in VEGA ZZ).
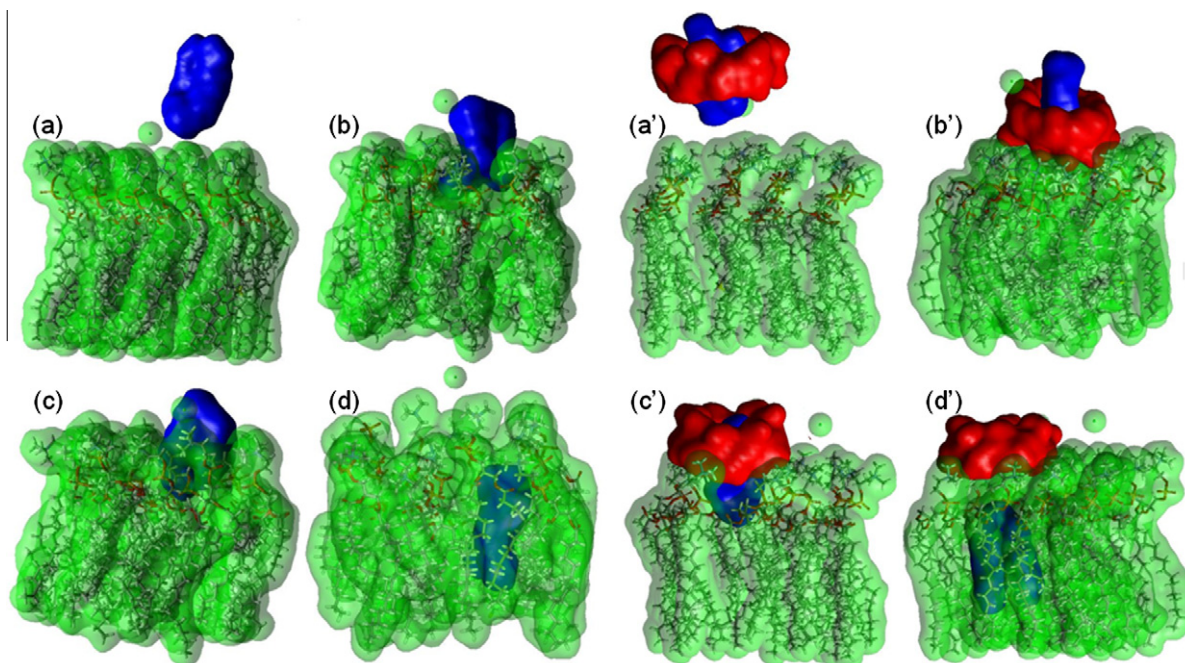
Fig. 5. Snapshots of the MD simulation as function of time for: (a, b, c and d) free [**DiC$_{10}$**] cation; (a′, b′, c′ and d′) β-**CD$_1$**·[**DiC$_{10}$**] inclusion complex in water. Water molecules and the inner phospholipids layer have been removed for clarity.

new step is observed: the complex must be dissociated before the insertion of [**DiC**$_{10}$] cation.

The other complexes remain in the aqueous external layer without adsorption onto the membrane model (not presented here). Indeed, the 2:1 complex remains in the external aqueous layer due to the absence of dipole moment (see Table 1). In these cases, the observed biocidal activity is only due to the various equilibria between free and complexed [**DiC**$_{10}$] cations. Therefore, the value of binding constants (i.e. the affinity of the [**DiC**$_{10}$] cation for the **CD**), the complex stoichiometry and geometry, the molecular properties (i.e. dipole moment) are key parameters to obtain a biocidal activity. Finally, one difference can be highlighted: for β-**CD**$_1$·[**DiC**$_{10}$] inclusion complex, when the [**DiC**$_{10}$] cation is inserted in the membrane model, the β-**CD** remains bound to the phospholipid layer (Debouzy et al., 1998; Fauvelle et al., 1997). This observation is probably at the origin of the MIC decrease observed for β-**CD**/[**DiC**$_{10}$] mixtures (see above, Fig. 2). Indeed, when the [**DiC**$_{10}$] cation is inserted into the cell membrane, the β-**CD**$_1$·[**DiC**$_{10}$] inclusion complex is only partially disrupted because the presence of the ammonium leads to a local modification of the cell membrane (see above: the ζ-potential). The effect is not sufficient to induce the cell lysis but allows maintaining the **CD** near the membrane, thus influencing the cell growth. This assumption is supported by the inefficiency of the **CD** alone because the membrane does not insert [**DiC**$_{10}$] cations (see above).

3.5. In vitro antifungal mechanism

To confirm experimentally the mechanism of the biocidal activity of the free [**DiC**$_{10}$] cation, we have recorded the mean colony count data (log$_{10}$ of the number of cfu/mL), the emf and the ζ-potential over time of aqueous suspensions of *C. albicans* with or without [**DiC**$_{10}$][**Cl**] (Figs. 6–8). It is noteworthy that the initial [**DiC**$_{10}$][**Cl**] concentration (C_A) is fixed at 5 (C_A < MIC), 50 (MIC < C_A < MBC) and 250 μM (MBC < C_A) (see Fig. 6). These concentrations are below the CMC (i.e. only unimers are present). Therefore, the emf can be easily converted in the free [**DiC**$_{10}$] concentration ([**DiC**$_{10}$]$_{free}$) from Eq. (1). Moreover, the ζ-potential evolution over time can be related to the cellular surface charge.

Without [**DiC**$_{10}$] cation, the *C. albicans* cell number remains constant (i.e. there is no cellular death or growth during the experience time). Moreover, the ζ-potential is not time dependent and its average mean is slightly negative (-2.4 ± 0.2 mV). Therefore, as described in the literature, the *C. albicans* membrane is globally negatively charged (Henriques et al., 2004). As depicted in Fig. 6, when 200 μM of [**DiC**$_{10}$] are added to the aqueous *C. albicans*

suspension, there is a clear relationship between the decrease of cells number and the decrease of the [**DiC**$_{10}$] concentration which confirms the antifungal activity of free [**DiC**$_{10}$] cations for concentrations above MBC. As the *C. albicans* membrane is negatively charged (see above), the free [**DiC**$_{10}$] cation decreasing is due to the insertion in the cell membrane. This insertion initiates the cell lysis. Moreover, the free [**DiC**$_{10}$] concentration decreases during the first minutes before to reach a plateau. The concentration difference between the initial concentration and the value obtained at the plateau is about 100 μM. This value confirms the MBC of free [**DiC**$_{10}$] cations obtained from the biocidal assays (79 ± 10 μM). More surprisingly, Fig. 6 shows a sharp decrease of the ζ-potential over time at 200 μM. The reduction of the ζ-potential is explained by an increase in the number of the chloride anions adsorbed on the cells due to the insertion of [**DiC**$_{10}$] cations in the membrane. Indeed, when [**DiC**$_{10}$] cations are intercalated between the phospholipids, the surface potential becomes more positive and some chlorides are adsorbed on the cell surface which decreases the ζ-potential (see above). Therefore, the loss of cell viability is due to the insertion of some [**DiC**$_{10}$] cations in the cell membrane which disrupts the surface cell potential that leads to a deterioration of the membrane. For a [**DiC**$_{10}$] concentration of 50 μM (i.e. a [**DiC**$_{10}$] concentration above the MIC and below the MBC), they is a slow decrease of the cell number compare to 200 μM. On the other part, there is a decrease of free [**DiC**$_{10}$] concentration (around 30 μM in one hour) and a sharp decrease of the ζ-potential. Therefore, the microorganism death kinetic rate is clearly dependant of the free [**DiC**$_{10}$] concentration. It is noteworthy that for concentration below the MIC (i.e. [**DiC**$_{10}$] <5 μM in Fig. 6), no significant change is observed for all quantities measured. All the results observed for *C. albicans* suspension with [**DiC**$_{10}$] cations are highly compatible with the proposed mechanism (see above).

Now, we can consider the antifungal mechanism of **CD**/[**DiC**$_{10}$] mixtures. The results are presented in Figs. 7 and 8 for MIC < C_A < MBC and MBC < C_A, respectively.

It is clear that for [**DiC**$_{10}$][**Cl**] total concentrations comprised between the MIC and the MBC, there is no or very weak cell lyses because all initial free [**DiC**$_{10}$] concentrations are lower than the MBC of free [**DiC**$_{10}$] cation (79 μM). The most interestingly results are observed for the ζ-potential behavior over time. Indeed, a clear decrease is observed for γ-**CD**/[**DiC**$_{10}$] mixture that can be related to the loss of free [**DiC**$_{10}$] cation due to the insertion of [**DiC**$_{10}$] cations in the cell membrane which disturbs the membrane potential and leads to microorganism growth inhibition. In contrast, for β-**CD**/[**DiC**$_{10}$] mixture, the ζ-potential increases due to the presence of **CDs**, in the vicinity of cells, which shielded the chloride negative
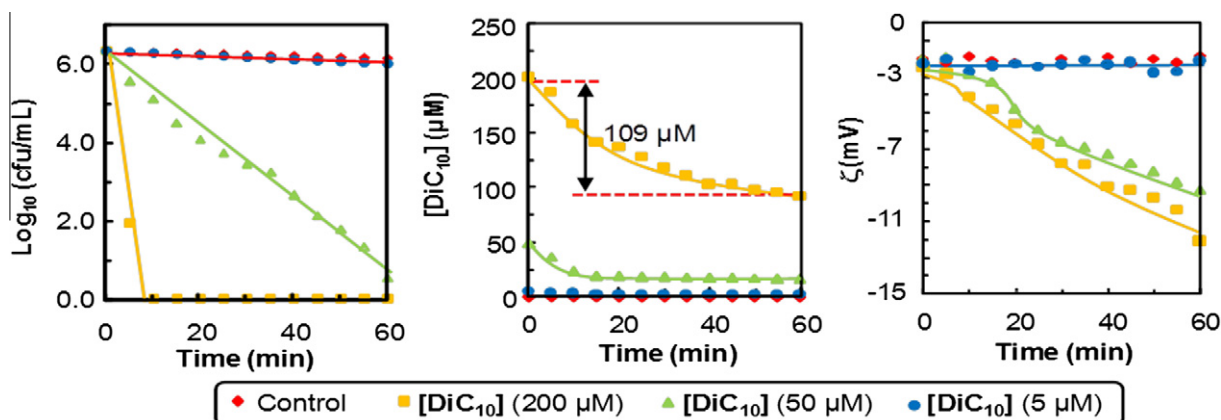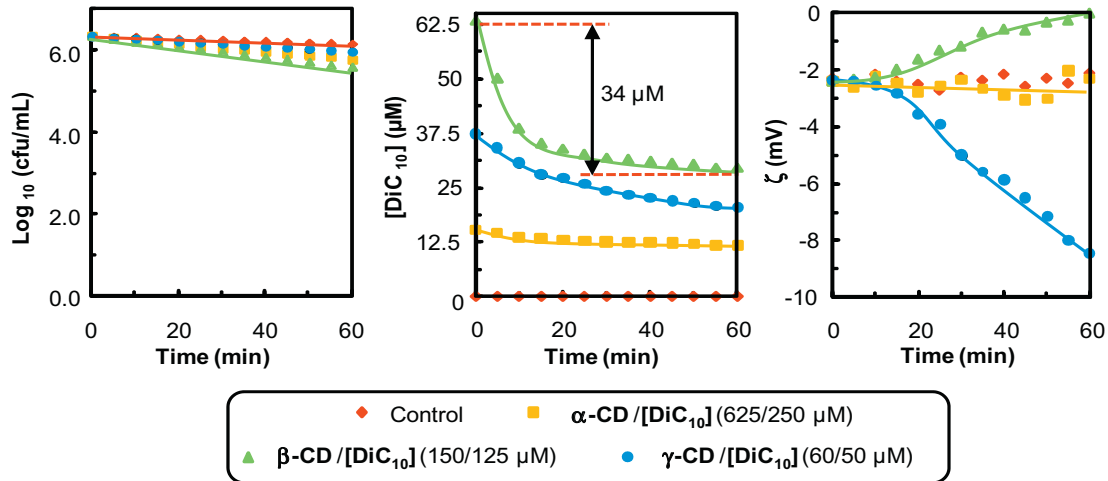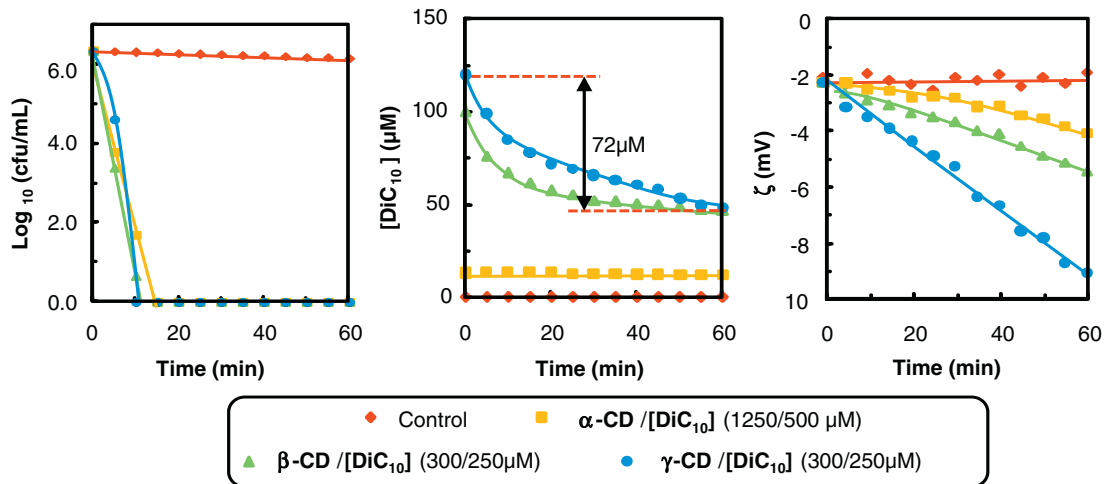

Fig. 6. Cell viability, free [**DiC**$_{10}$] concentration and ζ-potential as a function of time for *C. albicans* suspension at 20 ± 0.1 °C with various [**DiC**$_{10}$][**Cl**] total concentrations. The standard deviations are 16%, 8% and 3% for cell viability, ζ-potential and free [**DiC**$_{10}$] concentrations, respectively.

Fig. 7. Cell viability, free [**DiC$_{10}$**] concentration and ζ-potential as a function of time for *C. albicans* suspension at 20 ± 0.1 °C with various **CD** and [**DiC$_{10}$**][**Cl**] total concentrations. The [**DiC$_{10}$**][**Cl**] total concentration is comprised between the MIC and the MBC of the considered mixture. The standard deviations are 16%, 8% and 3% for cell viability, ζ-potential and free [**DiC$_{10}$**] concentration, respectively.

Fig. 8. Mean values for log$_{10}$ of the numbers of cfu/mL, free [**DiC$_{10}$**] concentration and ζ-potential vs. time for *C. albicans* suspension at 20 ± 0.1 °C with various **CD** and [**DiC$_{10}$**][**Cl**] total concentrations. The [**DiC$_{10}$**][**Cl**] total concentration is above the MBC of the considered mixture. The standard deviations are 16%, 8% and 3% for cell viability, ζ-potential and free [**DiC$_{10}$**] concentration, respectively.
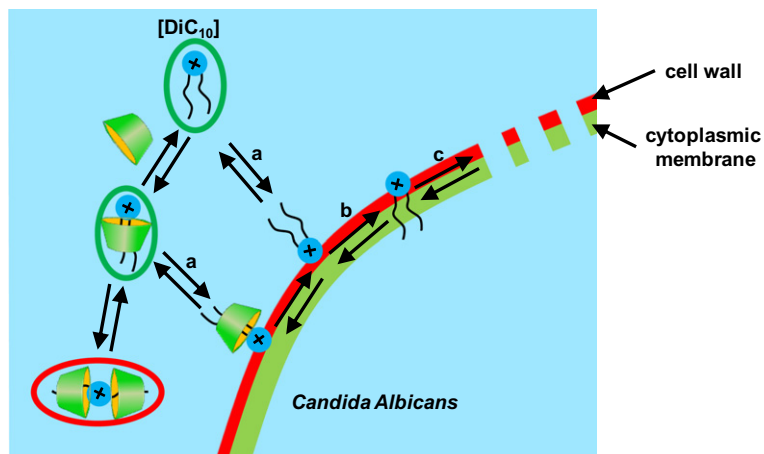
Fig. 9. Biocidal activity on *C. albicans* of various aggregates formed in **CD**/[**DiC$_{10}$**] mixtures: (a) electrostatic interaction of free or complexed [**DiC$_{10}$**] with the cell membrane, (b) insertion of [**DiC$_{10}$**] in the cell wall or cytoplasmic membrane, (c) cell wall and cytoplasmic membrane lysis. The green and red circles are active and inactive species in the mixture.

charges. For α-**CD**/[**DiC**$_{10}$] mixture, the ζ-potential remains constant due to the weak amount of free [**DiC**$_{10}$] cations inserted in the cell membrane.

As depicted in Fig. 8, when the [**DiC**$_{10}$][**Cl**] total concentrations are higher than the MBC of the considered mixtures, cell lyses occur. For β- and γ-**CD**/[**DiC**$_{10}$] mixtures, the initial free [**DiC**$_{10}$] concentrations (76 and 120 μM, respectively) are higher than the MBC of free [**DiC**$_{10}$] cation (79 μM): the biocidal activity (i.e. microorganism death) is due to a sufficient amount of free [**DiC**$_{10}$] cations. However, the initial free [**DiC**$_{10}$] concentration of α-**CD**/[**DiC**$_{10}$] mixture is lower than the MBC of free [**DiC**$_{10}$] cation (13 vs. 79 μM). The observed antifungal activity is due to a progressive release of [**DiC**$_{10}$] cations by the complexes. This assumption is corroborated by the loss of free ammonium cations: for α-**CD**/[**DiC**$_{10}$] mixture only 1 μM is lost. Therefore, it is clear that the complexed cations are released and directly incorporated in the cell membrane. The same behavior can be invoked for β-**CD**/[**DiC**$_{10}$] mixture: the ammonium loss is only 53 μM. For the γ-**CD**/[**DiC**$_{10}$] mixture, the ammonium loss is around 72 μM (i.e. the MBC of free [**DiC**$_{10}$] cations). Therefore, the biocidal activity of γ-**CD**/[**DiC**$_{10}$] mixture is only due to free [**DiC**$_{10}$] cations. It is noteworthy that γ-**CD** can complex only one [**DiC**$_{10}$] cation and that the association constant is weaker than the two other 1:1 complex (see Table 1). The ζ-potential behavior over time supports the proposed mechanisms. For the γ-**CD**/[**DiC**$_{10}$] mixture, the ζ-potential decrease is due to the free ammonium available in the solution. In contrast, the ζ-potential decrease weaker for the α-mixture and β-**CD**/[**DiC**$_{10}$] mixtures because the free **CD**s remain in the vicinity of the cell membrane. Indeed, when the total [**DiC**$_{10}$] concentration is above the MBC of the considered mixture, the amplitude of ζ-potential decrease is in the following order: free [**DiC**$_{10}$] cations (−9.6 mV) > γ-**CD**/[**DiC**$_{10}$] (−6.8 mV) > β-**CD**/[**DiC**$_{10}$] (−3.2 mV) > α-**CD**/[**DiC**$_{10}$] (−1.8 mV). The same behavior is observed when the total [**DiC**$_{10}$] concentration is comprised between the MIC and the MBC of the considered mixture. This observation can be used to explain the cell growth inhibition observed principally with α- and β-**CD**s (see the MIC values).

4. Conclusion

Antifungal properties of the double-tailed quaternary ammonium surfactant, di-*n*-decyldimethylammonium chloride, have been estimated by the measurement of the minimum biocidal concentrations (MBC) and minimum inhibitory concentrations (MIC) with or without α-, β- and γ-**CD**s. The results demonstrate that [**DiC**$_{10}$] cations, encapsulated in the **CD**, can act as efficient antifungal agents against *C. albicans*. The resulting activity is at least comparable to that of the free [**DiC**$_{10}$] depending on the **CD** choice. Moreover, for β-**CD**/[**DiC**$_{10}$] mixture, synergistic inhibition of cell growth is observed due to the presence of cyclodextrin in the vicinity of the cell membrane. The antifungal mechanism of free or encapsulated [**DiC**$_{10}$] biocide has been investigated from *in silico* (molecular properties calculation and molecular dynamics) and *in vitro* analyses (antifungal activity, potentiometry and zetametry). The proposed antimicrobial mechanism for **CD**·[**DiC**$_{10}$][**Cl**] complexes is based on the mechanism of free [**DiC**$_{10}$] cation with four-steps: (i) the positively-charged complex diffuses through the solution, (ii) it adsorbs onto the fungus membrane surface by electrostatic interaction, (iii) then it dissociates and the ammonium inserts into the microorganism membrane, and (iv) the change of the cell surface charge induces cell lysis (Fig. 9).

Besides the fact that cyclodextrins are biocompatible, they can be seen as reservoirs of the amphiphilic quaternary biocide avoiding at the same time, its spontaneous self-aggregation with polyethoxylated alcohols in detergent/disinfectant formulations

leading to a loss of efficiency. The developed approach can be generalized to other types of amphiphilic or organic biocides. Moreover, due to the current interest in the development of new biocidal formulations, work is currently underway in our laboratory to obtain more information on the self-assembly mechanism of [**DiC**$_{10}$] with **CD**s in the presence of surfactant mixtures such as polyethoxylated alcohols.

References

Arun, R., Ashok, K.C.K., Sravanthi, V.V.N.S.S., 2008. Cyclodextrins as drug carrier molecule: a review. Sci. Pharm. 76, 567–598.

Ashman, R.B., Blanden, R.V., Ninham, B.W., Evans, D.F., 1986. Interaction of amphiphilic aggregates with cells of the immune system. Immunol. Today 7, 278–283.

Balgavy, P., Devinsky, F., 1996. Cut-off effects in biological activities of surfactants. Adv. Colloid Int. Sci. 66, 23–63.

Cocera, M., Lopez, O., de la Maza, A., Parra, J.L., Esteerich, J., 1999. Electrokinetic study of the sublytic interaction of alkyl sulfates with phosphatidylcholine liposomes. Langmuir 15, 2230–2233.

Collinet-Fressancourt, M., Leclercq, L., Baudoin, P., Aubry, J.-M., Nardello-Rataj, V., 2011. Counter anion effect on the self-aggregation of dimethyl-di-*n*-octylammonium cation: a dual behavior between hydrotropes and surfactants. J. Phys. Chem. B 115, 11619–11630.

Cybulski, J., Wiśniewska, A., Kulig-Adamiak, A., Lewicka, L., Cieniecka-Rosłonkiewicz, A., Kita, K., Fojutowski, A., Nawrot, J., Materna, K., Pernak, J., 2008. Long-alkyl-chain quaternary ammonium lactate based ionic liquids. Chem. Eur. J. 14, 9305–9311.

Debouzy, J.C., Fauvelle, F., Crouzy, S., Girault, L., Chapron, Y., Göschil, M., Gadelle, A., 1998. Mechanism of α-cyclodextrin induced hemolysis 2. A study of the factors controlling the association with serine-, ethanolamine-, and choline-phospholipids. J. Pharm. Sci. 87, 59–66.

D'Enfert, C., Hube, B. (Eds.), 2007. Candida: Comparative and Functional Genomics. Caister Academic Press, Norfolk.

del Burgo, P., Aicart, E., Junquera, E., 2007. Mixed vesicles and mixed micelles of the cationic–cationic surfactant system: didecyldimethylammonium bromide/ dodecylethyl dimethylammonium bromide/water. Colloids Surf. A 292, 165–172.

Denyer, S.P., 1995. Mechanism of action antibacterial biocides. Int. Biodeter. Biodegr. 36, 227–245.

Fauvelle, F., Debouzy, J.C., Crouzy, S., Göschl, M., Chapron, Y., 1997. Mechanism of alpha-cyclodextrin-induced hemolysis. 1. The two-step extraction of phosphatidylinositol from the membrane. J. Pharm. Sci. 86, 935–943.

Ferraz, R., Branco, L.C., Prudêncio1, C., Noronha, J.P., Petrovski, Ž., 2011. Ionic liquids as active pharmaceutical ingredients. ChemMedChem 6, 975–985.

Funasaki, N., Ishikawa, S., Neya, S., 2008. Advances in physical chemistry and pharmaceutical applications of cyclodextrins. Pure Appl. Chem. 80, 1511–1524.

Funasaki, N., Neya, S., 2000. Multiple complexation of didecyldimethylammonium bromide and cyclodextrins deduced from electromotive force measurements. Langmuir 16, 5343–5346.

Gaillard, P., Carrupt, P.A., Testa, B., Boudon, A., 1994. Molecular lipophilicity potential, a tool in 3D QSAR method and application. J. Comput. Aided Mol. Des. 8, 83–96.

Henriques, M., Azeredo, J., Oliveira, R., 2004. Adhesion of *Candida Albicans* and *Candida dubliniensis* to acrylic and hydroxypatite. Colloids Surf. B 33, 235–241.

Hiramatsu, K., Kameyama, K., Ishiguro, R., Mori, M., Hayase, H., 2003. Properties of dilute aqueous solutions of double-chain surfactants, alkyldodecyldimethylammonium bromides with a change in the length of the alkyl chains. Bull. Chem. Soc. Jpn. 76, 1903–1910.

Hough, W.L., Smiglak, M., Rodríguez, H., Swatloski, R.P., Spear, S.K., Daly, D.T., Pernak, J., Grisel, J.E., Carliss, R.D., Soutullo, M.D., Davis, J.H., Rogers, R.D., 2007. The third evolution of ionic liquids: active pharmaceutical ingredients. New J. Chem. 31, 1429–1436.

Hough-Troutman, W.L., Smiglak, M., Griffin, S., Reichert, W.M., Mirska, I., Jodynis-Liebert, J., Adamska, T., Nawrot, J., Stasiewicz, M., Rogers, R.D., Pernak, J., 2009. Ionic liquids with dual biological function: sweet and anti-microbial, hydrophobic quaternary ammonium-based salts. New J. Chem. 33, 26–33.

Jeulin, H., Grancher, N., Kedzierewicz, F., Finance, C., Le Faou, A.E., Venarda, V., 2008. In vivo antiviral activity of ribavirin/α-cyclodextrin complex: evaluation on experimental measles virus encephalitis in mice. Int. J. Pharm. 357, 148–153.

Klamt, A., Schümann, G., 1993. COSMO: a new approach to dielectric screening in solvents with explicit expressions for the screening energy and its gradient. J. Chem. Soc. Perkin Transactions 2, 799–805.

Kopecký, F., Vojteková, M., Kovačová, S., Jurčeková, M., 2004. Inclusion complexation of carbethopendecinium bromide with some α- and β-cyclodextrins studied by potentiometry with membrane electrodes. Collect. Czech. Chem. Commun. 69, 384–396.

Kopecký, F., Vojteková, M., Vrana, M., Čížová, K., 2002. Potentiometric study of carbisocaine micellization and inclusion complexation with α-cyclodextrin, β-cyclodextrin, methyl-β-cyclodextrin, and (hydroxypropyl)-β-cyclodextrin collect. Czech. Chem. Commun. 67, 245–256.

Kopecký, F., Kopecká, B., Kaclík, P., 2001. Solubility study of nimodipine inclusion complexation with α- and β-cyclodextrin and some substituted cyclodextrins. J. Incl. Phenom. Macro. Chem. 39, 215–217.

Korth, M., 2010. Third-generation hydrogen-bonding corrections for semiempirical QM methods and force fields. J. Chem. Theory Comput. 6, 3808–3816.

Leclercq, L., Nardello-Rataj, V., Rauwel, G., Aubry, J.-M., 2010a. Structure-activity relationship of cyclodextrin/biocidal double-tailed ammonium surfactant host–guest complexes: towards a delivery molecular mechanism? Eur. J. Pharm. Sci. 41, 265–275.

Leclercq, L., Nardello-Rataj, V., Turmine, M., Azaroual, N., Aubry, J.-M., 2010b. Stepwise aggregation of dimethyl-di-n-octylammonium chloride in aqueous solutions: from dimers to vesicles. Langmuir 26, 1716–1723.

Leclercq, L., Lacour, M., Sanon, S.H., Schmitzer, A.R., 2009. Cyclodextrin sequestration: a new approach to efficient catalyst recovery. Chem. Eur. J. 15, 6327–6331.

Leclercq, L., Schmitzer, A.R., 2008. Multiple equilibria in the complexation of dibenzylimidazolium bromide salts by cyclodextrins: toward controlled self-assembly. J. Phys. Chem. B 112, 11064–11070.

Leclercq, L., Bricout, H., Tilloy, S., Monflier, E., 2007. Biphasic aqueous organometallic catalysis promoted by cyclodextrins: can surface tension measurements explain the efficiency of chemically modified cyclodextrins? J. Colloid Int. Sci. 307, 481–487.

Leclercq, L., Sauthier, M., Castanet, Y., Mortreux, A., Bricout, H., Monflier, E., 2005. Two-phase hydroformylation of higher olefins using randomly methylated α-cyclodextrin as mass transfer promoter: a smart solution for preserving the intrinsic properties of the rhodium/trisulfonated triphenylphosphine catalytic system. Adv. Synth. Catal. 347, 55–59.

Lehner, S.J., Müller, B.W., Seydel, J.K., 1993. Interactions between p-hydroxybenzoic acid esters and hydroxypropyl-β-cyclodextrin and their antimicrobial effect against Candida albicans. Int. J. Pharm. 93, 201–208.

Loftsson, T., Sigfusson, S.D., Sigurosson, H.H., Masson, M., 2003. The effects of cyclodextrins on topical delivery of hydrocortisone: the aqueous diffusion layer. STP Pharma Sci. 13, 125–131.

Mälkiä, A., Murtomäki, L., Urtti, A., Kontturi, K., 2004. Drug permeation in biomembranes: in vitro and in silico prediction and influence of physicochemical properties. Eur. J. Pharm. Sci. 23, 13–47.

Merianos, J.J., 2001. Surface-active agents in Disinfection, sterilization, and Preservation. In: Block, S.S. (Ed.). Lippincott Williams & Wilkins, Philadelphia, pp. 283–320.

Obłak, E., Lachowicz, T.M., Łuczyński, J., Witek, S., 2001. Comparative studies of the biological activities of lysosomotropic aminoesters and quaternary ammonium salts on the yeast Saccharomyces cerevisiae. Cell. Mol. Bio. Lett. 6, 871–880.

Pedretti, A., Villa, L., Vistoli, G., 2004. VEGA – an open platform to develop chem-bio-informatics applications, using plug-in architecture and script programming. J. Comput. Aided Mol. Des. 18, 167–173.

Pernak, J., Chwała, P., 2003. Synthesis and anti-microbial activities of choline-like quaternary ammonium chlorides. Eur. J. Med. Chem. 38, 1035–1042.

Pernak, J., Feder-Kubis, J., 2005. Synthesis and properties of chiral ammonium-based ionic liquids. Chem. Eur. J. 11, 4441–4449.

Pernak, J., Smiglak, M., Griffin, S.T., Hough, W.L., Wilson, T.B., Pernak, A., Zabielska-Matejuk, J., Fojutowski, A., Kita, K., Rogers, R.D., 2006. Long alkyl chain quaternary ammonium-based ionic liquids and potential applications. Green Chem. 8, 798–806.

Rahman, S.S., Simovic, I., Gibbons, S., Zloh, M., 2011. In silico screening for antibiotic escort molecules to overcome efflux. J. Mol. Model. 17, 2863–2872.

Rodenas, E., Dolcet, C., Valiente, M., Valerón, E.C., 1994. Physical properties of dodecyltrimethylammonium bromide (DTAB) micelles in aqueous solution and their behavior as the reaction medium. Langmuir 10, 2088–2094.

Rosen, M.J., 2004. Surfactants and interfacial phenomena, 3rd Edition. Wiley-Interscience, New York.

Russell, A.D., Hugo, W.B., Ayliffe, G.A.J., 1999. Principles and Practice of Disinfection, Preservation and Sterilization, thirdrd ed. Blackwell Science, Oxford.

Ryan, K.J., Ray, C.G. (Eds.), 2010. Sherris Medical Microbiology, 5th edition. McGraw Hill, New York.

Sabaté, R., Gallardo, M., Estelrich, J., 2000. Electrophoretic properties of dodecyltrimethylammonium bromide micelles in KBr solution. Electrophoresis 21, 481–485.

Schmidt, A., von der Eltz, H., Kaluza, K., 1996. US Pat. 5506216.

Simpson, W.J., 1992. Neutralization of the antibacterial action of quaternary ammonium compounds with cyclodextrins. FEMS Microbiol. Lett. 90, 197–200.

Stella, V.J., Rao, V.M., Zannou, E.A., Zia, V., 1999. Mechanisms of drug release from cyclodextrin complexes. Adv. Drug Deliv. Rev. 36, 3–16.

Stella, V.J., Rajewski, R.A., 1997. Cyclodextrins: their future in drug formulation. Pharmaceut. Res. 14, 556–567.

Šuljagić, V., 2008. Disinfection and Decontamination: Principles, Applications and Related issues. CRC Press, Boca-Raton, pp. 130–131.

Uekama, K., Hirayama, F., Irie, T., 1998. Cyclodextrin-based controlled drug release system. Chem. Rev. 98, 2045–2076.

Walsh, S.E., Maillard, J.-Y., Russell, A.D., Catrenich, C.E., Charbonneau, D.L., Bartolo, R.G., 2003. Activity and mechanisms of action of selected biocidal agents on Gram-positive and -negative bacteria. J. Appl. Microbiol. 94, 240–247.

Zloh, M., Gibbons, S., 2007. The role of small molecule-small molecule interactions in overcoming biological barriers for antibacterial drug action. Theor. Chem. Acc. 117, 231–238.